Heliyon 10 (2024) e35394

Contents lists available at ScienceDirect

Heliyon

journal homepage: www.cell.com/heliyon

Research article

Exploration of the pharmacological components and therapeutic mechanisms in treatment of Alzheimer's disease with Polygonati Rhizoma and its processed product using combined analysis of metabolomics, network pharmacology, and gut microbiota

Liao Xiaojuan [a,1], Liu Hongmei [a,1], Wang Zhuxin [a], Liu Xiaoqin [b], Deng Lanbing [a], Luo Dan [a], Zhou Yi [a,*]

[a] The Second Affiliated Hospital of Hunan University of Chinese Medicine, Changsha, 410005, China
[b] College of Pharmacy, Shandong Modern University, Jinan, 250104, China

ARTICLE INFO

Keywords:
Polygonati Rhizoma and its processed product
Alzheimer's disease
Therapeutic components and mechanisms
Gut microbiota
Network pharmacology

ABSTRACT

Polygonati Rhizoma (PR, Huangjing in Chinese) and its processed product (PRP), which are used in Traditional Chinese medicine (TCM) for cognitive enhancement and treatment of Alzheimer's disease (AD), have not been fully explored in terms of the different mechanisms underlying their anti-AD effects. Therefore, we used APP/PS1 mice as an AD model to assess the effects of PR and PRP on anxiety-like behaviors, cognitive function, memory performance, and pathological changes in the murine brain. UPLC-HRMS was applied to identify the components of PR and PRP that entered into the blood and brain. Network pharmacology was used to elucidate potential mechanisms underlying the improvement of AD. Differences in the intestinal flora composition between mice treated with PR and PRP were investigated using 16S rRNA sequencing, establishing a correlation between pharmacological components and distinct flora profiles. The results revealed that both PR and PRP interventions ameliorated cognitive deficits and attenuated Amyloid β (Aβ) plaque deposition in the brains of AD mice. Seven specific blood-entering components, namely glutamic acid, Phe-Phe, and uridine, etc., were associated with PR intervention, whereas ten specific blood-entering components including (2R,3S)-3-isopropylmalate, 3-methylhexahydropyrrolo[1,2-a]pyrazine-1,4-dione, and 3-methoxytyrosine were related to PRP intervention. Uridine was identified as a common brain-penetrating component in both PR and PRP interventions. Network pharmacology analysis suggested that the NOD-like receptor signaling pathway, Calcium signaling pathway and Alzheimer's disease were specific pathways targeted in AD treatment using PR intervention. Moreover, the apoptosis pathway was specifically linked to AD treatment during PRP intervention. Furthermore, the administration of both PR and PRP enhanced the abundance and diversity of the intestinal flora in APP/PS1 mice. Western blotting confirmed that PR excels in regulates inflammation, whereas PRP balances autophagy and apoptosis to alleviate the progression of AD. This study offers valuable insights and establishes a robust foundation for further comprehensive exploration of the intrinsic correlation between TCM and AD.

* Corresponding author. The Second Affiliated Hospital of Hunan University of Chinese Medicine. No. 233 Noth Cai'E Road, Changsha, 410005, China.
E-mail address: 226405736@qq.com (Z. Yi).
[1] Liao Xiaojuan and Liu Hongmei are co-first authors for this paper.

https://doi.org/10.1016/j.heliyon.2024.e35394
Received 8 April 2024; Received in revised form 20 June 2024; Accepted 28 July 2024
Available online 30 July 2024

1. Introduction

Alzheimer's disease (AD) is a neurodegenerative disorder primarily characterized by deficits in memory, cognition, language, and behavior [1]. The underlying pathogenesis of AD remains elusive; however, current understanding suggests its association with the extracellular deposition of Amyloid β (Aβ), leading to the formation of senile plaques [2], hyperphosphorylation of tau protein [3], neuronal and synaptic loss [4], inflammatory response within the nervous system [5,6], and aberrant cerebrovascular function [7]. The World Health Organization (WHO) estimates that the AD prevalence in the elderly population aged over 65 years ranges from 4 % to 7 %, whereas in those aged over 85 years, the prevalence can reach as high as 20 %–30 %. According to the assessment conducted by AD International (ADI), a staggering 75 % of individuals worldwide suffering from AD remain undiagnosed, while merely 21 % of AD patients in China have received a standardized diagnosis, including only 19.6 % who have undergone drug treatment. Currently, acetylcholine transferase blockers and N-methyl-D-aspartate receptor antagonists are commonly employed in the treatment of AD to ameliorate the disease and impede its progression [8,9]. Although they exhibit varying degrees of cognitive enhancement in patients with AD, the complete resolution of AD-related symptoms remains elusive because of their inherent limitations such as high toxicity, adverse effects, and suboptimal oral bioavailability [10,11]. Consequently, there is a pressing need for novel preventive and therapeutic agents which has emerged as a prominent area of research.

Traditional Chinese medicine (TCM), with its advantages of evidence-based treatment, holistic views, holistic regulation, multi-targeting, and individualized medication, has been confirmed by an increasing number of studies to have a positive impact on improving the symptoms of patients with AD, and its role in AD treatment has gradually received increased attention. The TCM medicinal Polygonati Rhizoma (PR, Huangjing in Chinese) and its processed product (PRP), the dried rhizome of *Polygonatum sibiricum* Red., were first documented in Miscellaneous Records of Famous Physicians *(Mingyi Bielu in Chinese*) (220–450 A.D.). They are long-standing and extensively used herbal medicines in TCM clinics for immune regulation, cognitive enhancement, and anti-AD effects mediated through oxidative stress, inflammation, fibrosis, lipid metabolism, apoptosis, and other signaling pathways [12].

Depending on the patient's symptoms, PR and its processed product, PRP (prepared by steaming raw PR in Chinese yellow rice wine), are commonly utilized as individual herbs or incorporated into compound prescriptions for the treatment of AD. The pathways through which PR and PRP mitigate AD symptoms are diverse. Notably, PR enhanced learning and memory in D-galactose-induced senescent rats [13]. Additionally, both PR and PRP exhibit a neuroprotective effect on the Aβ25-35 -induced PC12 cell injury model [14]. Moreover, PRP exerts antioxidant and anti-inflammatory effects by reducing oxidative stress in the brain. By activating the Wnt/β-catenin pathway, it regulates the balance of glycogen synthase kinase 3β (GSK-3β), protein phosphatase 2A (PP2A), and other enzyme activities. This leads to a decrease in Aβ content in the brain, attenuation of hyperphosphorylation of tau protein, as well as other multi-targeting effects that effectively alleviate neurological function symptoms while improving learning and memory abilities and exerting an anti-AD neuroprotective function. The main constituent of PR and PRP, *Polygonatum sibiricum* polysaccharides, exhibits the potential to enhance memory and cognitive deficits, mitigate synaptic loss, decrease the concentration of $A\beta_{1\text{-}40}$ and $A\beta_{1\text{-}42}$, alleviate intestinal inflammatory response in 5 X FAD mice [15]. Furthermore, it ameliorates cerebral tissue damage by reducing malondialdehyde levels in the mitochondria and plasma by augmenting mitochondrial antioxidant activity (e.g., manganese superoxide dismutase) [16]. In addition, it scavenges hydroxyl radicals and superoxide anions to attenuate neuronal cell apoptosis and cognitive function impairment [17]. Moreover, it inhibits apoptosis by modulating the B-cell lymphoma 2-associated X protein (Bax)/B-cell lymphoma 2 (Bcl-2) ratio and caspase-3 activation via the downregulation of Bcl-2 expression and upregulation of Bax expression. It also enhances the phosphatidylinositol 3 kinase (PI3K)/protein kinase B (Akt) signaling pathway [18]. Thus, both PR and PRP are therapeutic drugs for AD; however, the different pharmacological components and molecular mechanisms of action of PR and PRP against AD have not yet been verified, which restricts the clinical application of PR.

In this study, the APP/PS1 double transgenic mice were utilized as the AD model, and the effects of PR and PRP on locomotor and anxiety behaviors, as well as cognitive and memory levels in the mice, were observed through Morris water maze and open-field experiments. Pathological changes in brain tissues were examined using thioflavin-S staining method. Ultra-high performance liquid chromatography-high resolution mass spectrometry (UPLC-HRMS) was used to identify the chemical components of PR and PRP and those effective into the blood and brain. Network pharmacology was used to reveal potential mechanisms for improving AD. Differences in intestinal flora composition between mice treated with raw and processed PR were investigated using 16S rRNA sequencing, and the correlation between pharmacological components and differing flora was established. Western blotting method was used to verify differences in pharmacological mechanisms of action between PR and PRP. This study conducted a preliminary investigation into the disparities in the pharmacological constituents and biological mechanisms of PR and PRP in AD treatment, thereby offering insights and establishing a foundation for further comprehensive exploration of the intrinsic correlation between TCM and AD metabolism.

2. Materials and methods

2.1. Preparation of aqueous extracts of PR and PRP

The dried rhizomes of the *Polygonatum sibiricum* Red., obtained from Shanxi Yuanhe Tang Chinese Medicine Co., Ltd., Shanxi, China, were identified as PR and PRP herbal materials (batch numbers: 220212 and 220315, respectively) by Associate Chief Pharmacist Yi Zhou of the Second Affiliated Hospital of Hunan University of Chinese Medicine. Voucher specimens (voucher numbers: SXTCM-zhou-2023015 and SXTCM-zhou-2023016) were deposited in the Herbarium of the Shanxi College of Traditional Chinese

Medicine (SXTCM), Taiyuan, China.

Two hundred grams of PR and PRP were soaked in distilled water for 30 min, followed by the addition of eight times the volume of distilled water, heated under reflux for 40 min, and filtered to collect the extract. The residue was treated with six times the volume of distilled water, reheated under reflux for 40 min, and filtered. The extracts from both steps were combined and concentrated under reduced pressure at 50 °C to produce water extracts of PR and PRP with a concentration of 1 g·mL-1, stored at 4 °C for *in vivo* experiments.

2.2. Materials

C57BL/6J and APP/PS1 mice [(SPF (Beijing) Biotechnology Co., Ltd. Animal License No.: SCXK (Beijing) 2019-0010] were used, with the following features: SPF grade; three months old; body mass, 28 ± 3 g; male. The mice were free to drink and ingest food and were acclimatized under the following conditions for one week: temperature, 25 ± 2 °C; relative humidity, 55 ± 5 %; illumination conditions, 12 h light/12 h dark cycle. The experiments were approved by the Ethics Committee of the Second Affiliated Hospital of Hunan University of Chinese Medicine (approval number: 2023-KY-048) and conducted according to the Animal Research: Reporting of In *Vivo* Experiments guidelines.

2.3. AD mice model preparation and drug administration

After one week of acclimatization, eight C57BL/6J mice were used as the normal group (Normal), and APP/PS1 mice were randomly divided into the model group (Control), the low and high-dose raw PR group (PRL, 5 g kg^{-1}; PRH, 15 g kg^{-1}), and the low and high-dose dose processed PR group (PRPL, 5 g kg^{-1}; PRPH, 15 g kg^{-1}), with each group containing eight mice (the dosage was determined according to the conversion of body surface area between mice and humans and the previous study). The drug was administered by gavage (the Normal and Control groups were gavaged with the same volume of pure water) for four weeks.

2.4. AD mice behavioral assay

To evaluate the locomotor state, anxiety behavior, and cognitive and memory levels of the mice, the Morris water maze and open-field experiments were conducted sequentially with reference to a previous study by our team to determine the spatial memory ability of the mice in each group, record the evasion latency, number of times the mice traversed the platforms, and residence time in the target quadrant, and assess the cognitive and memory levels of the mice [19].

After the behavioral experiments, mice were anesthetized by inhalation with isoflurane, their blood was collected from the abdominal aorta and centrifuged (4000 g, 15 min, 4 °C), and the serum was collected and placed in the refrigerator at −80 °C for preservation and later use. Brain tissues were taken; one part of the brain tissue samples was placed in 10 % formalin for fixation, and another part was placed in −80 °C for preservation, to validate the anti-AD components of PR and PRP and evaluate the difference between their anti-AD mechanisms [20].

2.5. Thioflavin-S staining

Intact brain tissues were fixed in 4 % paraformaldehyde and incubated in 30 % sucrose solution at 4 °C overnight for dehydration; after embedding and coagulation, the sections were cut into frozen sections with a thickness of 30 μm; the sections were stained with 1 % thioflavin solution at room temperature for 5 min and rinsed twice with 50 % ethanol, each time for 5 min. A small amount of 50 % ethanol was dripped on the tissue area to keep the sections moist, and then the sections were placed under a fluorescence microscope (Nikon Ti–S, Tokyo, Japan).

2.6. UPLC-HRMS

Preparation of PR and PRP sample solution: 0.6 g of A concentrated solution of raw and processed PR was taken, placed in a centrifuge tube (2 mL) to which 0.4 g a methanol solution was added and vortexed to mix. Afterward, 600 μL of 40 % aqueous methanol solution was added to 200 μL of the mixture to dilute it; the resulting solution was then vortexed to mix and centrifuged (4 °C, 16 000 g, 15 min), and the supernatant was collected.

Preparation of serum sample: 100 μL of the serum sample was taken, upon which 400 μL of methanol was added; the resulting solution was vortexed to mix for 60 s, and then the mixture was left to stand at −20 °C for 30 min and centrifuged (4 °C, 16 000 g, 20 min); finally, the supernatant was taken for vacuum drying. Afterward, the residue was mixed with 50 μL of 40 % methanol aqueous solution, vortexed, and centrifuged (4 °C, 16 000 g, 15 min), and the supernatant was collected.

Preparation of blank serum + PR and PRP: 200 μL of the blank serum was taken, upon which 33.4 μL of raw PR and processed PR test solution was added. Subsequently, 800 μL of methanol was added, and the resulting solution was vortexed to mix for 60 s, and then the mixture was left to stand at −20 °C for 30 min and centrifuged (4 °C, 16 000 g, 20 min); finally, the supernatant was taken for vacuum-drying. The residue was then mixed with 100 μL of 40 % aqueous methanol, vortexed, and centrifuged, and the supernatant was collected.

Referring to previous omics studies by our team and literature reports, the chemical components in serum/brain tissues before and after the administration of PR and PRP were detected using the UHPLC-HRMS method and XCMS online software (http://xcmsonline.

scripps.edu). Secondary mass spectra (MS2) were compared, with an MS2 fragment similarity score greater than 0.7 as the screening criterion. The high-content components of PR and PRP were also identified. Next, high-content components whose peak response intensity in mouse serum/brain tissue after administration was more than three times that in the serum/brain tissue of AD control mice were selected for comparative analysis of the blood/brain-entering components of raw versus processed PR [21,22].

2.7. Network pharmacology analysis

Based on the results of the blood/brain-entering component analysis in section 2.6, we obtained the pharmacodynamic components of raw and processed PR. The Traditional Chinese Medicine Systems Pharmacology Database and Analysis (TCMSP) (https://old.tcmsp-e.com/tcmsp.php), Traditional Chinese Medicine Integrative Database (TCMID) (http://www.megabionet.org/tcmid/), and Comparative Toxicogenomics Database (CTD) (http://ctdbase.com/), were searched for relevant targets was conducted using both Chinese and English versions of PR, PRP, and AD as keywords. Gene names were harmonized using the UniProt (https://www. uniprot.org/) database. The intersection of the potential action targets of the compounds and disease targets was used to identify the potential action targets of the active components of TCM for AD treatment. Screening was performed based on the median gene degree median by drawing a venn diagram. Targets larger than the median were included to identify key disease targets with higher relevance. The key targets were imported into the String (https://cn.string-db.org/) database to obtain protein interactions, the network topology analysis of component-target-disease was performed, and the relevant network diagrams were drawn using the NetworkX software package (networkx-2.8.2, https://networkx.org). Gene Ontology (GO) and Kyoto Encyclopedia of Genes and Genomes (KEGG) analyses were performed using the GO (geneontology.org) and KEGG (https://www.kegg.jp/) databases, and the results of the pathway enrichment analysis were visualized using the R language, comparing and speculating on the differences in treatment networks and biological effect pathways involved in the pharmacological components of PR and PRP in AD treatment.

2.8. Intestinal flora analysis

Mouse fecal samples were collected, and DNA was extracted to assess its purity and concentration, followed by PCR amplification and purification. An Illumina Nova high-throughput sequencing platform was used to sequence the V3–V4 regions of the 16S rRNA gene in each sample. Sequence analysis was performed using the QIIME software (version 1.8.0), with UCLUST used for the dechimerization of high-quality sequences; then, sequences were clustered into operational taxonomic units (OTUs) at 97 % similarity. Abundance curves were generated based on OTU abundance distribution, and α diversity indices (Observed Species, Shannon, Simpson, Chao 1, ACE, Coverage, and PD whole tree) were calculated. Principal coordinate analysis (PCoA) was conducted on the preprocessed community data to understand the similarities and differences in the microbial community structures between the different samples. LEfSe analysis was conducted to identify the members that differed significantly between the sample communities. Furthermore, the significantly differential members whose linear discriminant analysis effect sizes were greater than 2 are presented in diagrams to show the strength of their effects. The Phylogenetic Investigation of Communities by Reconstruction of Unobserved States (PICRUSt) software was used to predict microbial metabolic functions based on species composition information obtained from the 16S sequencing data [23].

2.9. Western blotting

Total proteins were extracted from mouse brain tissues, and the expression levels of proteins such as Nuclear factor κB(NF-κB) (p65), phosphorylated Nuclear factor κB (p–NF–κB)(p65), NOD-like receptor protein 3 (NLRP3), phosphorylatedMammalian Target of Rapamycin (*p*-mTOR), Mammalian Target of Rapamycin (mTOR), sequestosome 1 (p62), B-cell lymphoma 2 (Bcl-2), and B-cell lymphoma 2-associated X-protein (Bax) were detected by the usual operating methods.

2.10. Statistical analyses

Data are presented as the mean ± standard errors of the mean (SEM) of three independent experiments. Differences between groups were identified using One-Way Analysis of Variance (ANOVA) with Tukey's post-hoc test using GraphPad Prism (version 6.0; GraphPad Software, La Jolla, CA, USA). $P < 0.05$ was considered statistically significant.

3. Results

3.1. Both PR and PRP improve cognitive deficits and reduce Aβ plaque deposition in the brain tissue of AD mice

To investigate the alleviation of AD pathological signs and differences in mice treated with PR and PRP, we used the Morris water maze and open-field behavioral experiments to observe mouse escape latency, platform crossing frequency, dwell time in the target quadrant, total movement time in the open field, movement distance in the central area, and corner movement time. Pathological changes in the brain tissue were also examined. The results were as follows:

In the Morris water maze experiment, compared with the Normal group, mice in the Control group had significantly longer escape latency ($P < 0.0001$), and significantly less time spent in the target quadrant ($P < 0.001$), swimming speed ($P < 0.0001$), and number of times crossing the platform ($P < 0.01$). Compared with the Control group, the escape latency of mice in each dosing group (Day 1: *P*

<0.05 in Donepezil group, $P<0.01$ in PRL group; Day 2: $P<0.0001$ in Donepezil, PRL, and PRH groups, respectively; Day 3: $P<0.05$ in Donepezil group, $P<0.001$ in PRL group, $P<0.0001$ in PRH group; Day 4: $P<0.01$ in PRL group, $P<0.0001$ in PRH group; Day 5: $P<0.05$ in Donepezil and PRPL groups, $P<0.01$ in PRH group; $P<0.001$ in PRPH group) were significantly shorter, and the target quadrant dwell time ($P<0.01$ for the PRPL group), swimming speed ($P<0.001$ for the PRPL group; $P<0.0001$ for the PRPH group), and the number of times crossing the platform ($P<0.05$ for the PRH group and $P<0.01$ for the PRPL and PRPH groups) were

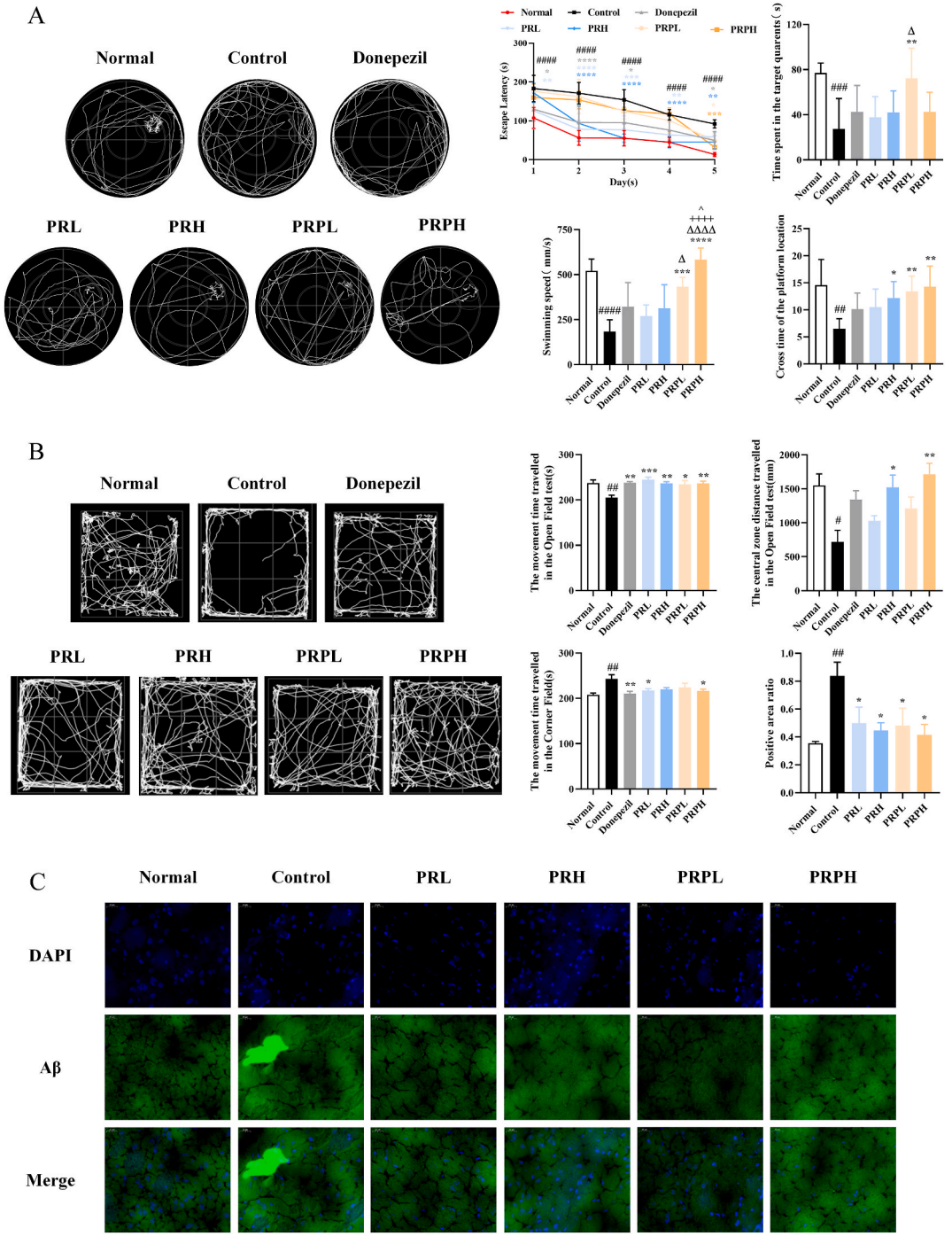

Fig. 1. Effects of PR and PRP on physiological indexes of AD mice.
Notes: Morris water maze (A), open-field tests (B), and Thioflavin-S staining (C) in AD mice. $^{\#}P<0.05$, $^{\#\#}P<0.01$, $^{\#\#\#}P<0.001$, $^{\#\#\#\#}P<0.0001$ *vs.* Normal group; $^{*}P<0.05$, $^{**}P<0.01$, $^{***}P<0.001$, $^{****}P<0.0001$ *vs.* Control group; $^{\Delta}P<0.05$ *vs.* PRL group; $^{+}P<0.05$, $^{++}P<0.01$ *vs.* PRH group; $\hat{}P<0.05$ *vs.* PRPL group; $^{\bigtriangledown}P<0.05$ *vs.* PRPH group.

significantly longer. Compared to the PRL group, the mice had a significantly longer target quadrant dwell time ($P < 0.05$ in the PRPL group) and swimming speed ($P < 0.05$ in the PRPL group; $P < 0.0001$ in the PRPH group). Swimming speed ($P < 0.0001$ for the PRPH group) was significantly prolonged in mice compared with that in the PRH group.

In the open-field experiment, compared with the Normal group, mice in the Control group exhibited a significant decrease in total movement time ($P < 0.01$) and the distance traveled in the center area ($P < 0.05$), and a significant prolongation of corner movement time ($P < 0.01$). Compared with the Control group, total movement time ($P < 0.05$ in the PRPL group; $P < 0.01$ in the Donepezil group, the PRH group, and the PRPH group; $P < 0.001$ in the PRL group) and central region movement distance ($P < 0.05$ in the PRH group; $P < 0.01$ in the PRPH group) were significantly prolonged in each dosing group of mice, and corner movement time ($P < 0.05$ for the PRL and PRPH groups; $P < 0.01$ for the Donepezil group) was significantly shorter.

Aβ plaque deposition is a characteristic pathological feature of AD. Thioflavin-S staining results revealed an increased area of intensely stained bright green plaques in the brain tissues of mice in the Control group compared to those in the Normal group, indicating a significant upregulation in Aβ protein expression ($P < 0.01$). Conversely, the various dosing groups exhibited a substantial reduction in the area of bright green plaques when compared with that observed in the Control group ($P < 0.05$) (Fig. 1).

3.2. Differential components analysis of PR and PRP

The collected data were imported into the local standardized spectrum database of traditional Chinese medicine for secondary mass spectrum search and comparison. A total of 51 classes of chemical components of PR were identified, among which the top six included benzene and its substituted derivatives, carboxylic acids and their derivatives (e.g. 2,2-diethylglycine, threonine, and phenylalanine), fatty acyls (e.g., (2R,3S)-3-isopropylmalate), indoles and its derivatives (e.g. L-tryptophan), organonitrogen compounds, and organooxygen compounds (e.g. pantothenate); 61 classes of components of processed PR were identified, of which the top six included benzene and its substituted derivatives, carboxylic acids and their derivatives (e.g. L-benzylalanine, threonine, and 3-methylhexahydropyrrolo [1,2-a]pyrazine-1,4-dione), fatty acyls (e.g., adipic acid, (2R,3S)-3-isopropylmalate), indoles and its derivatives (e.g., L-tryptophan), organooxygen compounds (e.g., 1-(4-Hydroxyphenyl)-2-methylaminoethanone), and phenols. Threonine, L-tryptophan, propan-2-yl 6-O-(4-carboxy -3-hydroxy-3-methylbutanoyl)-.beta.-D-glucopyranoside, citric acid, pidolic acid, succinic acid, uridine, (2R,3S)-3-isopropylmalate, and N- *trans*-coumaroyloctopamine and other saccharides and amino acids are the common carbohydrate and amino acid components common to both raw and processed PR (Table A. 1).

3.3. Different blood and brain-entering prototype components of PR and PRP analysis in AD mice

The components with high PR and PRP contents were identified by comparison with the secondary mass spectrometry database. The results revealed that PR exhibited 27 chromatographic peaks in base peak chromatography (BPC), with 12 peaks observed in positive-ion BPC and 15 peaks in negative-ion BPC (Fig.A.1). In contrast, PRP displayed 29 peaks, comprising 15 peaks in the positive-ion BPC and 14 peaks in the negative-ion BPC (Fig.A.1).

Serum chromatograms were compared among the AD mice treated with PR and PRP and the control mice, deducting endogenous components in serum, and analyzing the blood-entering chemical components of PR. The results indicated the following: adenosine, threonine, glutamic acid, Phe-Phe, N-acetyl-L-tyrosine, 3-(2R,3S)-3-isopropylmalate, and uridine are the seven components specific to PR; (2R,3S)-3-isopropylmalate、3-methylhexahydropyrrolo [1,2-a]pyrazine-1,4-dione、5-[(2,4- difluorophenoxy)methyl]-2-furoic acid, epiligulyl oxide, 1,2,3,4-butanetetrol, 1-(2-quinoxalinyl)-L,L-cyclo(leucylprolyl), 2-carboxythieno [3,2-b]benzothiophene, 4-hydroxy-3a,4,7,7a-tetrahydro-1H-isoindole-1,3(2H)-dione, corylifolinin, and 3-methoxytyrosine are 10 unique blood-entering components of PRP (Table 1).

Table 1
Identifying the therapeutic constituents of PR and PRP serum prototypes with potential anti-AD properties.

No.	*m/z*	RT/min	ppm	Compound name	Score	PR	PRP
1	268.1039	1.12	0.7	Adenosine	0.9999	Into Blood	None
2	102.0553	1.45	1.5	Threonine	0.9977	Into Blood	None
3	130.0498	2.26	0.7	Glutamic acid	0.9999	Into Blood	None
4	313.1543	4.97	1.2	Phe-Phe	0.9968	Into Blood	None
5	180.0659	1.26	3.8	N-Acetyl-L-tyrosine	0.9944	Into Blood	None
6	111.0078	1.55	10	3-Furoic acid	0.9995	Into Blood	None
7	243.0620	1.65	0.6	Uridine	0.9660	Into Blood	None
8	175.0605	2.45	4.1	(2R,3S)-3-Isopropylmalate	0.8356	None	Into Blood
9	169.0971	1.79	0.4	3-Methylhexahydropyrrolo [1,2-a]pyrazine-1,4-dione	0.9719	None	Into Blood
10	125.0233	2.01	0.5	5-[(2,4-Difluorophenoxy)methyl]-2-furoic acid	0.9732	None	Into Blood
11	213.1233	2.50	18.6	Epiligulyl oxide	0.7887	None	Into Blood
12	251.1028	4.00	1.2	1,2,3,4-Butanetetrol, 1-(2-quinoxalinyl)-	0.9245	None	Into Blood
13	211.1441	4.69	0.5	L,L-Cyclo(leucylprolyl)	0.9644	None	Into Blood
14	188.9857	1.41	10.4	2-Carboxythieno [3,2-b]benzothiophene	0.9716	None	Into Blood
15	184.0606	2.64	2.7	4-Hydroxy-3a,4,7,7a-tetrahydro-1H-isoindole-1,3(2H)-dione	0.9990	None	Into Blood
16	323.1348	3.21	18	Corylifolinin	0.8246	None	Into Blood
17	210.0768	4.27	0.4	3-Methoxytyrosine	0.9674	None	Into Blood

Analysis of the brain-entering chemical components of PR and PRP in AD mice after administration showed that uridine was the common brain-entering component of PR and PRP, while three components, including threonine, epiligulyl oxide, and L,L-cyclo (leucylprolyl) were the PRP-specific brain-entering components (Table 2).

3.3.1. The key component-core target-pathway network constructed for AD treatment using PR and PRP

Network pharmacological analysis was performed to construct a key component-core target-pathway network diagram by integrating all the blood/brain-entering components of PR and PRP, as described in Section 3.2. The number of potential targets of PR and PRP were identified as 582 and 221, respectively, after collection, screening and de-duplication, and de-emphasis, with a total of 17 967 AD-related genes collected in the CTD database. Intersecting component targets and disease targets, we obtained 530 potential targets for the PR treatment of AD and 220 potential targets for the PRP treatment of AD (Fig. 2A and B); for the common targets with a gene degree greater than the median, the protein-protein interaction (PPI) network was obtained through the String database, and 537 nodes and 2541 edges were included in the PPI network of raw PR; the PPI network of PRP contained 220 nodes and 1673 edges. Topology analysis was performed on the component-target-disease network using the top 50 targets as the core target (selecting all if the intersections were less than 50) (Fig. 2C–E). Pathway function annotation and pathway enrichment analysis of core targets were performed using the KEGG platform, and the results showed that the core targets were involved in 105 KEGG pathway-related entries. The data of the top 20 targets were analyzed according to the P value ($P < 0.05$). Based on the component-core target data and the results of the KEGG pathway analysis of the top 20 targets and a key component-core target-pathway network diagram, it was found that the CXC chemokine family, CASP3, TNF, MAPK1, MAPK3, and IL18 are the common potential targets for the treatment of AD by PR and PRP. Furthermore, the Toll-like receptor signaling pathway, Chagas disease (American trypanosomiasis), rheumatoid arthritis, toxoplasmosis, cytokine-cytokine receptor interaction, Hepatitis C, the MAPK signaling pathway, and pathways in cancer are the common signaling pathways of PR and PRP for AD treatment. The chemical composition of the blood/brain-entering components differed between raw and processed PR, as did their targets and pathways. EDN1, CHRM1, and CRH are unique potential targets of PR in AD treatment, whereas, AKT1, mTOR, JUN, CASP9, and TLR4 were the unique potential targets of PRP for AD treatment. NOD-like receptor signaling, long-term depression, chemokine signaling, amoebiasis, melanogenesis, gap junctions, epithelial cell signaling in *Helicobacter pylori* infection, gastric acid secretion, the GnRH signaling, axon guidance, AD, and the calcium signaling are pathways specific to PR in AD treatment. Bladder cancer, endometrial cancer, colorectal cancer, prostate cancer, pancreatic cancer, glioma, chronic myeloid leukemia, Leishmaniasis, melanoma, small cell lung cancer, apoptosis, and osteoclast differentiation are the inflammatory and apoptotic pathways specific to PRP in AD treatment (Fig. 2F and G).

3.4. Analysis of the effects of PR and PRP on the intestinal flora of AD mice

OTUs with 97 % similarity were selected for clustering, and the Venn diagram results showed that there were 3636 OTUs, of which 1349 were in the Normal group, 1437 in the Control group, 1368 in the PR group, and 1372 in the PRP group, for a total of 345 in the four groups (Fig. 3A).

In the phylum *Firmicutes*, *Bacteroidota*, *Actinobacteriota*, and *Desulfobacterota* accounted for more than 95 % of the total bacteria. The relative abundance of *Patescibacteria and Proteobacteria* were higher in the Control group than in the Normal group, and the relative abundance of *Patescibacteria* and *Proteobacteria* was lower in the PR and PRP groups than in the Control group. At the class level, the abundance of *Actinobacteria* was lower and the abundance of *Saccharimonadia* was higher compared with that of the Normal group; the abundance of *Actinobacteria* was higher and the abundance of *Saccharimonadia* was lower in the PR and PRP groups compared with the Control group. At the order level, the abundance of *Lachnospirales* and *Lactobacillales* was lower in the Control group than in the Normal group, but the abundance increased after PR and PRP treatment. At the family level, the abundance of *Lactobacillaceae* was lower and the abundance of *Rikenellaceae* and *Saccharimonadaceae* was higher than that of the Normal group; after treatment with PR and PRP, the abundance of *Lactobacillaceae* increased and the abundance of *Rikenellaceae* and *Saccharimonadaceae* decreased than that of the Control group. At the genus level, the abundance of *uncultured* and *Enterorhabdus* was lower compared to that in the Normal group; after treatment with PR and PRP, the abundance of both *uncultured* and *Enterorhabdus* increased than that of the Control group. At the species level, the abundance of *uncultured bacterium* decreased and then increased after treatment with PR and PRP, compared to that in the Control group (Fig. 3B). The results indicated that both raw and processed PR affected the species composition and relative abundance of mouse intestinal flora at the phylum, class, order, family, genus, and species levels.

The results of the α-diversity analysis showed that the ACE, Chao 1, coverage, observed species, Shannon, and Simpson indices increased and the PD whole tree index was lower in the Control group than in the Normal group; however, after PR and PRP

Table 2
Identifying the therapeutic constituents of PR and PRP brain prototypes with potential anti-AD properties.

No.	*m/z*	RT/min	ppm	Compound name	Score	PR	PRP
1	102.0553	1.45	1.5	Threonine	0.9977	None	Into Tissue
2	243.0621	1.65	0.6	Uridine	0.9660	Into Tissue	Into Tissue
3	213.1234	2.49	18.6	Epiligulyl oxide	0.7887	None	Into Tissue
4	211.1441	4.67	0.8	L,L-Cyclo(leucylprolyl)	0.9827	None	Into Tissue

Note: *m/z*: parent ion mass-to-charge ratio; RT/min: retention time/min; ppm: mass accuracy; Into Blood or None: the compound is in the blood or not; Into Tissue or None: the compound is in the brain or not.

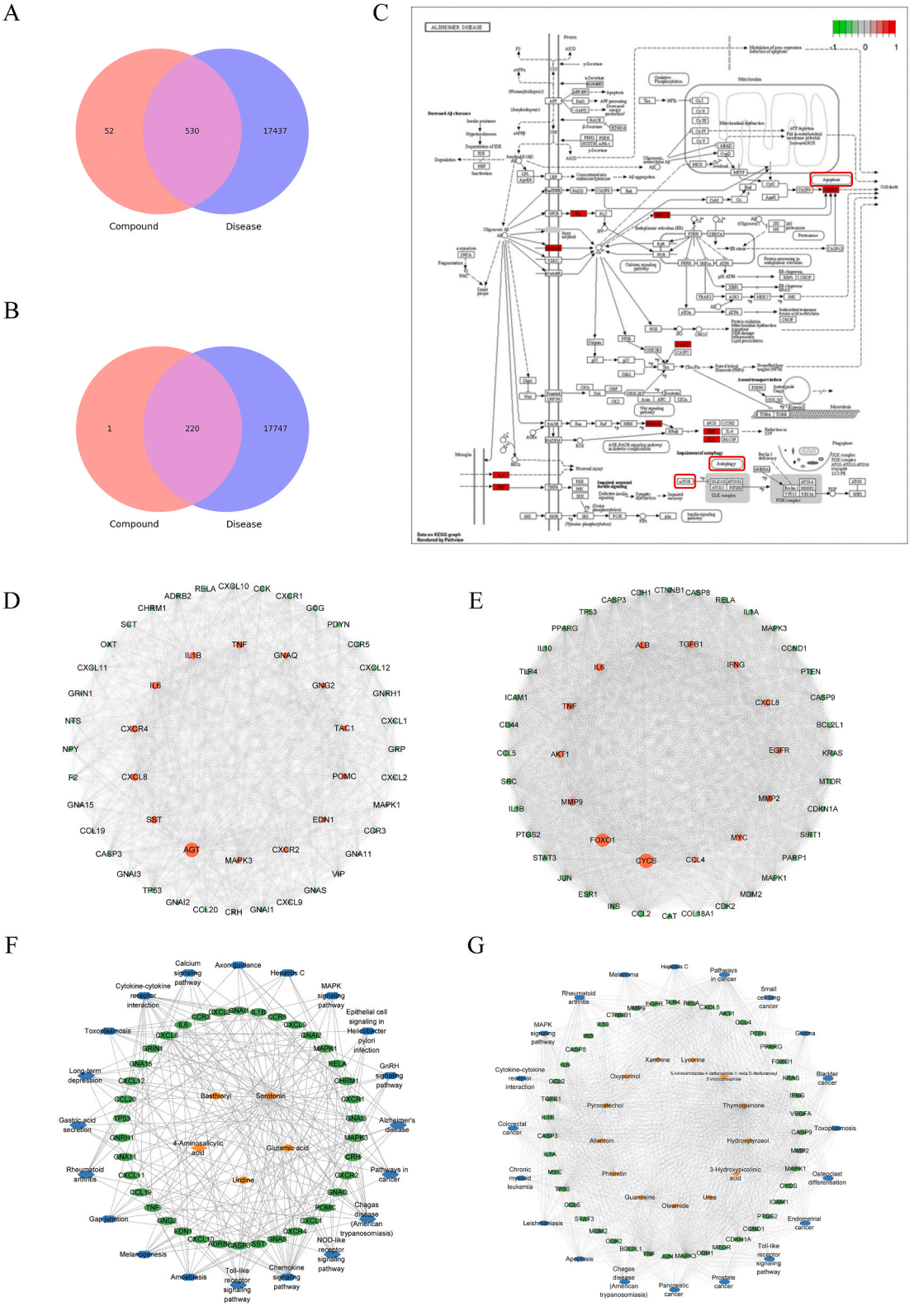

(caption on next page)

Fig. 2. The construction of key component-core target-pathways networks of PR and PRP on AD.
Notes: Venn diagram of PR (A), PRP (B) and disease targets; Alzheimer's disease signaling pathway (C) (https://www.kegg.jp/pathway/hsa05010); Core target (top 50) network diagram of PR (D) and PRP (E); Compound-Target-Pathway network diagrams (top 20) illustrating the therapeutic effects of active components in PR (F) and PRP (G) on AD.

interventions were given, compared to the Control group, the ACE, Chao 1, coverage, observed species, Shannon, and Simpson indices decreased, and the PD whole tree index increased in the Normal group (Fig. 3C).

Beta diversity analysis showed that the Bray Curtis index, Weighted Unifrac index, and Unweighted UnifracBeta index were elevated in the Control group compared to those in the Normal group. After the PR and PRP interventions, the Bray Curtis index, Weighted Unifrac index, and Unweighted UnifracBeta index decreased compared to those in the Control group (Fig. 3D). Principal Component Analysis (PCA), PCoA, and Non-metric Multidimensional Scaling (NMDS) analyses showed differences among the four groups. This was consistent with the Venn diagram results, indicating that both raw and processed PR interventions elevated the intestinal flora richness and diversity in mice (Fig. 3E). The results indicated that both raw and processed PR enhanced the diversity of the intestinal flora in mice. Enrichment analysis revealed that cell growth and death, amino acid metabolism, nervous system, and glycan biosynthesis and metabolism were the differential metabolic pathways between the Normal and Control groups. Nucleotide metabolism, metabolism of other amino acids, and membrane transport are the potential pathways of action of PR and PRP in AD treatment (Fig. 4A–C).

3.5. Correlation analysis

The R language was used to construct correlation coefficients between significant differential flora and significant blood/brain-entering components of PR and PRP in AD treatment. The results showed that Phe-Phe correlated most strongly with uncultured cells in the PR treatment, whereas L,L-cyclo(leucylprolyl) correlated most strongly with Bifidobacterium in the PRP treatment (Fig. 4D and E).

3.6. Differences of the inflammation, autophagy, and apoptosis related protein expression levels in the brain tissues of AD mice between PR and PRP

The expression levels of p–NF–κB(p65)/NF-κB(p65), NLRP3, *p*-mTOR/mTOR, p62, and Bcl-2/Bax in mouse brain tissues (Fig. 5) were examined by using western blotting to investigate the differential action mechanisms of PR and PRP on inflammation, autophagy, and apoptosis in AD mouse brain tissues.

Compared to the Normal group, the expression levels of p–NF–κB (p65)/NF-κB(p65) ($P < 0.05$) and NLRP3 ($P < 0.05$) were significantly elevated in the Control group. Comparing with the Control group, each administration group showed significant reduction in p–NF–κB (p65)/NF-κB(p65) (PRH, $P < 0.05$), NLRP3 (PRH, $P < 0.05$), and NLRP3 (PRL, $P < 0.01$) expression levels, respectively. Furthermore, compared to the PRPH group, there was a notable decrease in NLRP3 expression level in the PRL group ($P < 0.05$).

Compared to the Normal group, the Control group exhibited a significant increase in the expression levels of *p*-mTOR/mTOR ($P < 0.01$) and a significant decrease in the expression levels of p62 ($P < 0.05$). Compared to the Control group, *p*-mTOR/mTOR (PRH, $P < 0.05$; PRPL, $P < 0.01$) showed a significant decrease in expression levels, whereas p62 demonstrated significant increase in expression levels (PRPL and PRPH, $P < 0.05$). Moreover, compared to the PRL group, both PRPL and PRPH groups displayed significantly increased expression levels of p62 ($P < 0.05$).

Compared to the Normal group, the Control group exhibited significant decreases in the expression levels of Bcl-2/Bax ($P < 0.001$). All drug-administered groups showed significant increases in the expression levels of Bcl-2/Bax (PRPH) compared to the Control group ($P < 0.05$). Additionally, compared with the PRL group, the PRPH group demonstrated significant increase in the expression levels of Bcl-2/Bax ($P < 0.05$).

The above results indicate that both PR and PRP could alleviate the brain lesions in AD mice to different degrees via regulating inflammation, autophagy, and apoptosis, but PR was better at regulating inflammation to alleviate the symptoms in AD mice, while PRP was better at regulating the balance of autophagy and apoptosis to alleviate the symptoms in AD mice.

4. Discussion

PR and PRP have a rich pharmacological profiles and an extensive historical record their clinical utilization for medicinal and dietary purposes [24]. The primary chemical constituents of PR include polysaccharides, steroidal saponins, quinones, alkaloids, lignans, vitamins, and various amino acids [25]. The chemical components of PR and PRP were characterized using UPLC-HRMS technology in this experiment. The obtained experimental results confirmed that the processing led to alterations in the levels of polysaccharide (such as propan-2-yl 6-O-(4-carboxy-3-hydroxy-3-methylbutanoyl)-β-D-glucopyranoside and ethyl 4-O-(4-carboxy-3-hydroxy-3-methylbutanoyl)-β-D-glucopyranoside) and amino acids (such as Ala-Ile, Tyr-Phe, and Ser-Leu) present in PR.

The prevalence of AD is escalating rapidly, making it one of the most lethal and economically burdensome illnesses to manage in this era [26]. Currently, it is mainly used to delay the occurrence and development of AD by enhancing cognitive ability [27], alleviating neuropsychiatric symptoms [28], improving neuroinflammation [29], and targeting nerve protection; development of AD, no

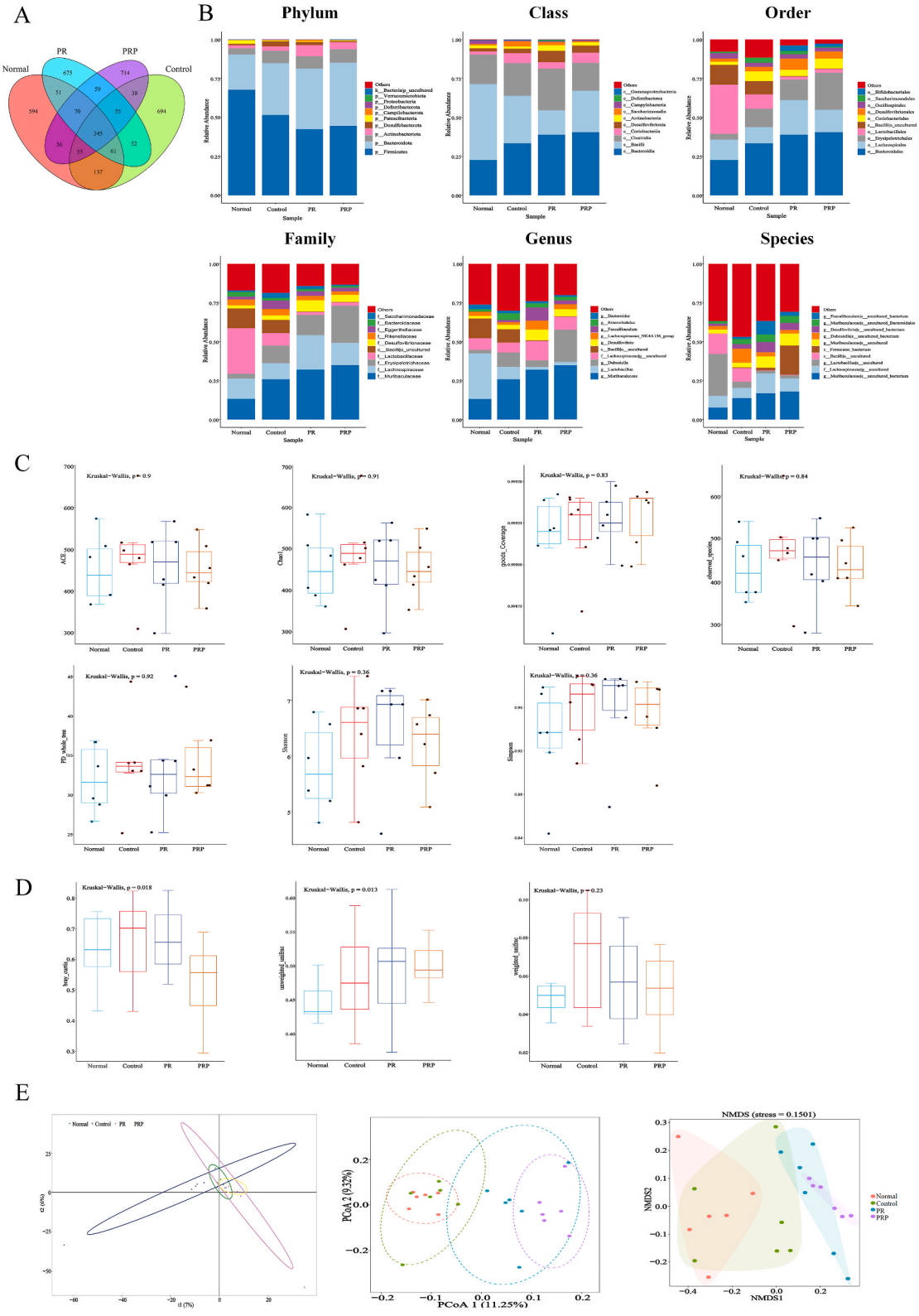

Fig. 3. Differential effect of PR and PRP on the gut microbiota of AD mice (n = 6).
Notes: A: ASV Venn; B: Map of community structure components; C: α diversity index difference analysis between groups; D: Analysis of β diversity between groups; E: Principal Component Analysis, Principal Co-ordinates Analysis and Non-Metric Multi-Dimensional Scaling.

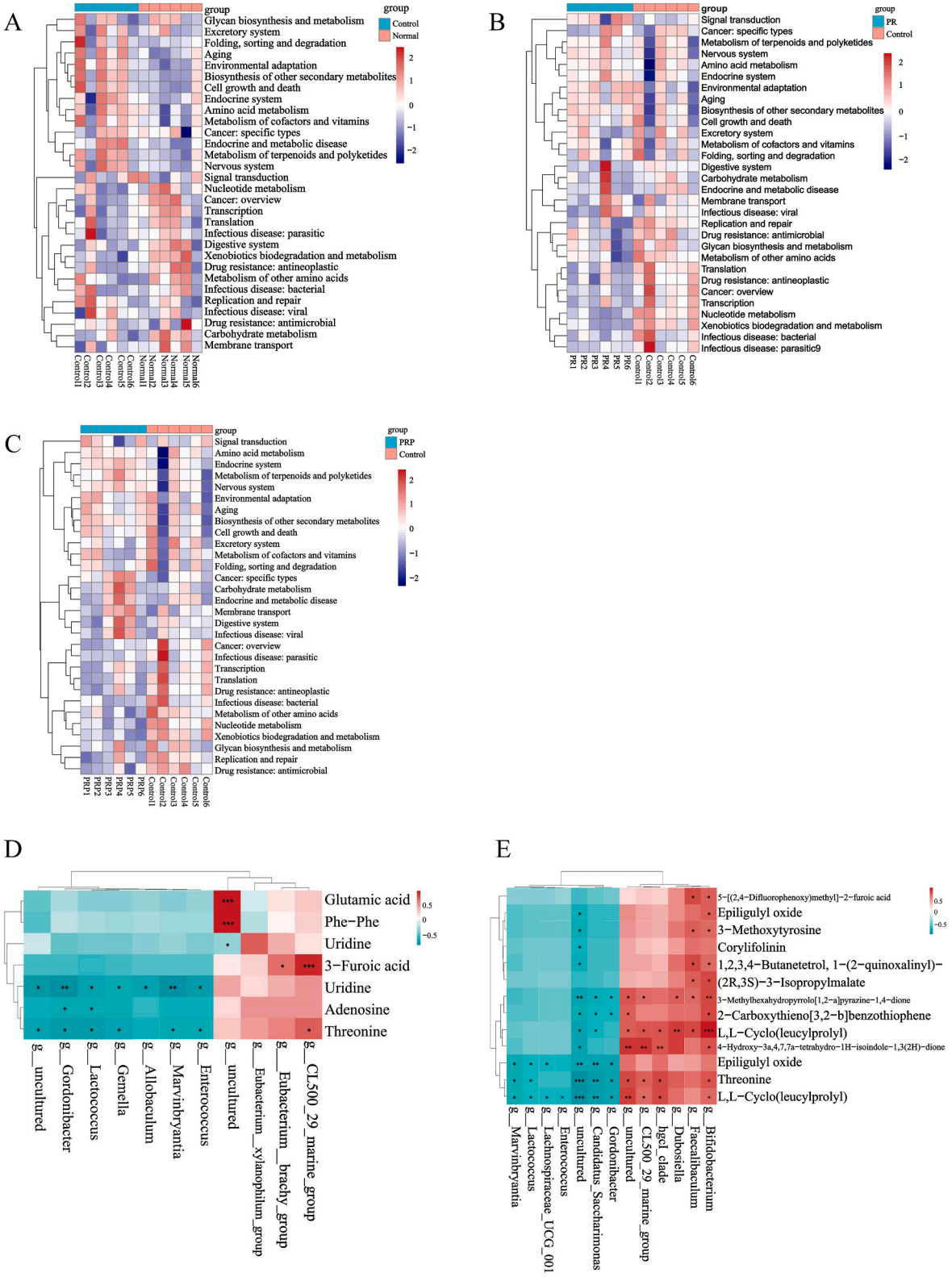

Fig. 4. The diagram of KEGG pathway enrichment analysis and Correlation analysis.
Notes: KEGG pathway enrichment analysis diagram of Normal and Control (A), PR and Control (B), PRP and Control (C). PR (D) and PRP (E) in the blood/brain components and a 16S correlation heat map.

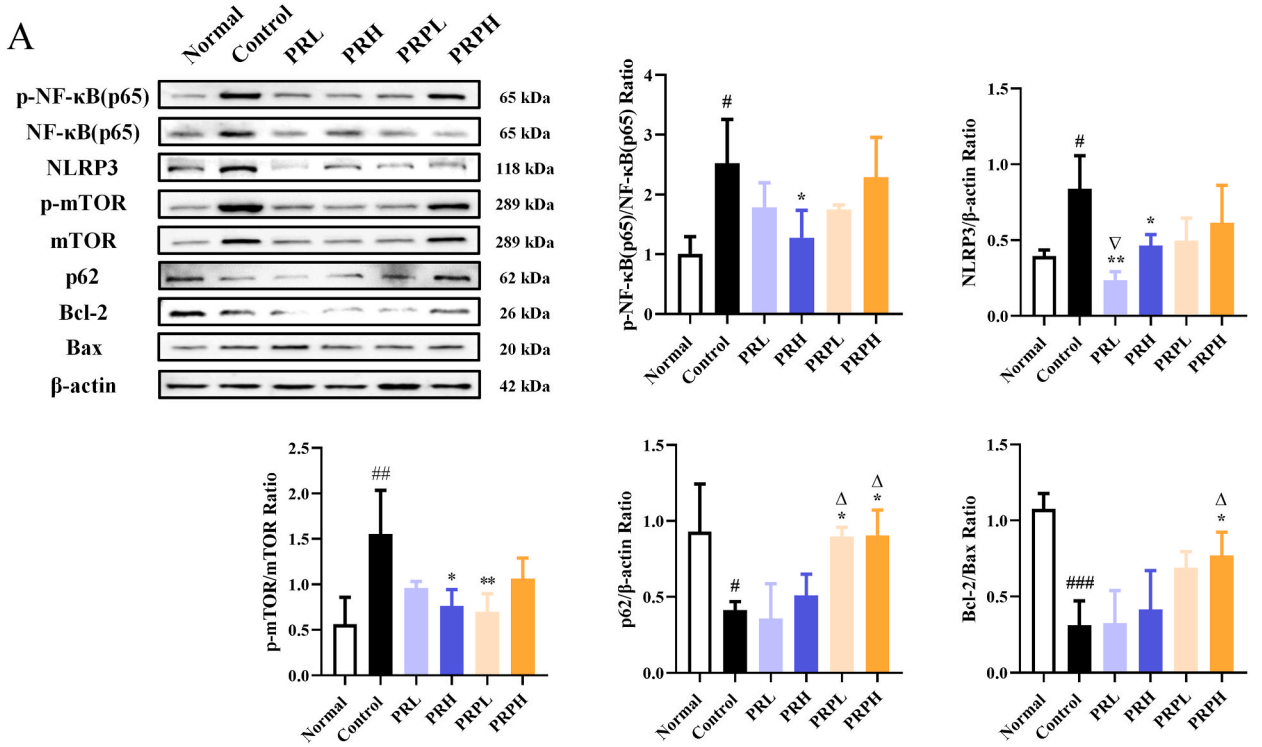

Fig. 5. Differential effects of PR and PRP on expression levels of inflammation, autophagy and apoptosis related proteins in brain of AD mice ($\bar{x} \pm s$, n = 3).
Notes: $^{\#}P < 0.05$, $^{\#\#}P < 0.01$ *vs.* Normal group; $^{*}P < 0.05$, $^{**}P < 0.01$ *vs.* Control group. $^{\Delta}P < 0.05$ *vs.* PRL group; $^{\nabla}P < 0.05$ *vs.* PRPH group.

cure has been found [30]. PR treatment can exert pharmacological effects such as antioxidant and anti-aging effects [31], immunity regulation [32], and memory improvement through various signaling pathways such as oxidative stress, inflammation, lipid metabolism, and apoptosis [12]. *Polygonatum sibiricum* polysaccharides have antioxidant properties and promotes learning and memory ability in D-galactose-induced senescent rats [13,33]. In this experiment, the UPLC-HRMS technique was used to identify the pharmacodynamic components of raw and processed PR that entered the blood/brain, and the related experimental results confirmed the followings: raw and processed PR improved the pathological state of Aβ plaque deposition in the brain of AD mice; the spatial learning and memory ability of AD mice improved. Seven blood-entering components, including adenosine, threonine, glutamic acid, Phe-Phe, and uridine, were specific to raw PR; whereas 10 blood-entering components, including (2R,3S)-3-isopropylmalate, 3-methylhexahydropyrrolo [1,2-a]pyrazine-1,4-dione, and 3-methoxytyrosine, were specific to processed PR. Uridine was a brain-entering component common to both raw and processed PR, whereas threonine, epiligulyl oxide, and L,L-cyclo(leucylprolyl) are the brain-entering components specific to processed PR. Although the chemical components of both raw and processed PR, as well as their blood/brain-entering components, were identified in this experiment, the results showed that most of them were sugars and amino acids. Aqueous extracts of raw and processed PR were selected for the subsequent *in vivo* experiments to treat AD mice and investigate the differential molecular mechanisms of raw and processed PR in AD treatment.

AD patients have cognitive dysfunction and neuroinflammatory responses in the brain [34], decreased autophagy [35], and apoptosis [36] play essential roles in this process. With the continuous aging of the brain tissue, a large amount of reactive oxygen species and free radicals are generated on the neuronal cell membrane, which in turn induces lipid peroxidation, leading to damage to the cell membrane structure and function; this leads to calcium ion overload, and an increase in the level of inflammatory factors within the brain tissue, resulting in inflammatory responses in the central nervous system. Long-term oxidative stress induces a neuronal toxicity cascade and the formation of amyloid plaques, which are extremely difficult to dissolve, thus aggravating the inflammatory reactions in the nervous system and activating calcium-dependent proteases, lipases, and kinases, leading to excessive Tau protein phosphorylation. Excessive Tau protein phosphorylation leads to neurofibrillary tangles and neuronal damage in the brain, thus aggravating cognitive impairment. In this experiment, western blotting was used to verify that PR and PRP differently regulate inflammation, autophagy, and apoptosis in mouse brain tissues, and that raw PR is better at regulating inflammation to alleviate the symptoms in AD mice, while processed PR is better at regulating the balance of autophagy and apoptosis to alleviate the symptoms of AD mice. However, this study did not investigate the differential molecular mechanisms of raw and processed PR; we did not verify the relevant molecular mechanism using in vitro cellular experiments; we also did not detect the expression level of the relevant genes using quantitative real-time PCR, which needs to be further studied.

5. Conclusions

In this study, we conducted a preliminary investigation into the disparities in the pharmacological constituents and biological mechanisms of PR and PRP in AD treatment, thereby offering insights and establishing a foundation for further comprehensive exploration of the intrinsic correlation between TCM and AD metabolism.

Funding

This work was supported by the projects Hunan Province Natural Science Foundation (No.2021JJ80063), Key research project of Hunan Province Traditional Chinese Medicine Administration (No.A2023033), and The seventh batch of national traditional Chinese medicine experts inherit academic experience studio.

Data availability

Data will be made available on request.

Ethics declarations

The animal study protocol was approved by the Animal Care and Use Committee of the Second Affiliated Hospital of the Hunan University of Chinese Medicine (approval number:2023-KY-048).

Consent for publication

Not applicable.

Patient consent for publication

Not applicable.

Abbreviations

AD	Alzheimer's disease
ADI	Alzheimer's Disease International
Akt	Protein kinase B
Aβ	Amyloid β-protein
Bax	B-cell lymphoma 2-associated X-protein
Bcl-2	B-cell lymphoma 2
BPC	Base Peak Chromatography
CTD	Comparative Toxicogenomics Database
DNA	Deoxyribonucleic Acid
GO	Gene Ontology
GSK-3β	Glycogen Synthase Kinase 3β
KEGG	Kyoto Encyclopedia of Genes and Genomes
LEfSe	Linear discriminant analysis Effect Size
mTOR	Mammalian Target of Rapamycin
NF-κB (p65)	Nuclear factor κB (p65)
NLRP3	NOD-like receptor protein 3
OTUs	Operational Taxonomic Units
PCA	Principal component analysis
PCoA	Principal coordinate analysis
PCR	Polymerase Chain Reaction
PI3K	Phosphatidylinositol 3 kinase
PICRUSt	The phylogenetic Investigation of Communities by Reconstruction of Unobserved States
p-mTOR	PhosphorylatedMammalian Target of Rapamycin
p–NF–κB (p65)	Phosphorylated Nuclear factor κB (p65)
PP2A	Protein Phosphatase 2A
PPI	Protein-Protein Interaction network
PR	*Polygonatum sibiricum* Red.
PRP	*Polygonatum sibiricum* Red. Processed product
RNA	Ribosomal Ribonucleic Acid
TCM	Traditional Chinese medicine
TCMID	Traditional Chinese Medicine integrative database
TCMSP	Traditional Chinese Medicine Systems Pharmacology Database and Analysis
UPLC-HRMS	Ultra-high-performance liquid chromatography high-resolution mass spectrometry
WHO	The World Health Organization

CRediT authorship contribution statement

Liao Xiaojuan: Writing – review & editing, Writing – original draft, Funding acquisition, Formal analysis, Data curation, Conceptualization. **Liu Hongmei:** Writing – review & editing, Writing – original draft, Formal analysis, Data curation, Conceptualization. **Wang Zhuxin:** Formal analysis, Data curation. **Liu Xiaoqin:** Writing – original draft, Methodology, Investigation, Formal analysis, Data curation. **Deng Lanbing:** Formal analysis, Data curation, Conceptualization. **Luo Dan:** Data curation, Conceptualization. **Zhou Yi:** Writing – review & editing, Writing – original draft, Methodology, Investigation, Funding acquisition, Formal analysis, Data curation, Conceptualization.

Declaration of competing interest

The authors declare that they have no known competing financial interests or personal relationships that could have appeared to influence the work reported in this paper.

Acknowledgments

Not applicable.

Appendix A. Supplementary data

Supplementary data to this article can be found online at https://doi.org/10.1016/j.heliyon.2024.e35394.

References

[1] A. Johri, Disentangling mitochondria in Alzheimer's disease, Int. J. Mol. Sci. 22 (21) (2021 Oct 26) 11520, https://doi.org/10.3390/ijms222111520.
[2] A. González, S.K. Singh, M. Churruca, R.B. Maccioni, Alzheimer's disease and tau Self-Assembly: in the search of the Missing Link, Int. J. Mol. Sci. 23 (8) (2022 Apr 10) 4192, https://doi.org/10.3390/ijms23084192.
[3] J.A. Pradeepkiran, M. Munikumar, A.P. Reddy, P.H. Reddy, Protective effects of a small molecule inhibitor ligand against hyperphosphorylated tau-induced mitochondrial and synaptic toxicities in Alzheimer disease, Hum. Mol. Genet. 31 (2) (2021 Dec 27) 244–261, https://doi.org/10.1093/hmg/ddab244.
[4] K. Lao, R. Zhang, J. Luan, Y. Zhang, X. Gou, Therapeutic strategies targeting amyloid-β receptors and Transporters in Alzheimer's disease, J Alzheimers Dis 79 (4) (2021) 1429–1442, https://doi.org/10.3233/JAD-200851.
[5] R.B. Maccioni, L.P. Navarrete, A. González, A. González-Canacer, L. Guzmán-Martínez, N. Cortés, Inflammation: a Major target for compounds to control Alzheimer's disease, J Alzheimers Dis 76 (4) (2020) 1199–1213, https://doi.org/10.3233/JAD-191014.
[6] F. Yin, H. Sancheti, I. Patil, E. Cadenas, Energy metabolism and inflammation in brain aging and Alzheimer's disease, Free Radic. Biol. Med. 100 (2016 Nov) 108–122, https://doi.org/10.1016/j.freeradbiomed.2016.04.200.
[7] H. Zhou, F. Gao, X. Yang, T. Lin, Z. Li, Q. Wang, Y. Yao, L. Li, X. Ding, K. Shi, Q. Liu, H. Bao, Z. Long, Z. Wu, R. Vassar, X. Cheng, R. Li, Y. Shen, Endothelial BACE1 Impairs cerebral small Vessels via Tight junctions and eNOS, Circ. Res. 130 (9) (2022 Apr 29) 1321–1341, https://doi.org/10.1161/CIRCRESAHA.121.320183.
[8] M. Saxena, R. Dubey, Target enzyme in Alzheimer's disease: Acetylcholinesterase Inhibitors, Curr. Top. Med. Chem. 19 (4) (2019) 264–275, https://doi.org/10.2174/1568026619666190128125912.
[9] Y. Ju, K.Y. Tam, Pathological mechanisms and therapeutic strategies for Alzheimer's disease, Neural Regen Res 17 (3) (2022 Mar) 543–549, https://doi.org/10.4103/1673-5374.320970.
[10] L. Pinheiro, C. Faustino, Therapeutic strategies targeting amyloid-β in Alzheimer's disease, Curr. Alzheimer Res. 16 (5) (2019) 418–452, https://doi.org/10.2174/1567205016666190321163438.
[11] S. Tiwari, V. Atluri, A. Kaushik, A. Yndart, M. Nair, Alzheimer's disease: pathogenesis, diagnostics, and therapeutics, Int J Nanomedicine 14 (2019 Jul 19) 5541–5554, https://doi.org/10.2147/IJN.S200490.
[12] P. Zhao, C. Zhao, X. Li, Q. Gao, L. Huang, P. Xiao, W. Gao, The genus Polygonatum: a review of ethnopharmacology, phytochemistry and pharmacology, J. Ethnopharmacol. 214 (2018 Mar 25) 274–291, https://doi.org/10.1016/j.jep.2017.12.006.
[13] S. Zheng, Protective effect of Polygonatum sibiricum Polysaccharide on D-galactose-induced aging rats model, Sci. Rep. 10 (1) (2020 Feb 10) 2246, https://doi.org/10.1038/s41598-020-59055-7.
[14] X. Yang, Y. Guan, B. Yan, Y. Xie, M. Zhou, Y. Wu, L. Yao, X. Qiu, F. Yan, Y. Chen, L. Huang, Evidence-based complementary and alternative medicine bioinformatics approach through network pharmacology and molecular docking to determine the molecular mechanisms of Erjing pill in Alzheimer's disease, Exp. Ther. Med. 22 (5) (2021 Nov) 1252, https://doi.org/10.3892/etm.2021.10687.
[15] S. Luo, X. Zhang, S. Huang, X. Feng, X. Zhang, D. Xiang, A monomeric polysaccharide from Polygonatum sibiricum improves cognitive functions in a model of Alzheimer's disease by reshaping the gut microbiota, Int. J. Biol. Macromol. 213 (2022 Jul 31) 404–415, https://doi.org/10.1016/j.ijbiomac.2022.05.185.
[16] Z. Zhang, B. Yang, J. Huang, W. Li, P. Yi, M. Yi, W. Peng, Identification of the protective effect of *Polygonatum sibiricum* polysaccharide on d-galactose-induced brain ageing in mice by the systematic characterization of a circular RNA-associated ceRNA network, Pharm. Biol. 59 (1) (2021 Dec) 347–366, https://doi.org/10.1080/13880209.2021.1893347.
[17] F. Shen, Z. Song, P. Xie, L. Li, B. Wang, D. Peng, G. Zhu, Polygonatum sibiricum polysaccharide prevents depression-like behaviors by reducing oxidative stress, inflammation, and cellular and synaptic damage, J. Ethnopharmacol. 275 (2021 Jul 15) 114164, https://doi.org/10.1016/j.jep.2021.114164.
[18] X. Cui, S. Wang, H. Cao, H. Guo, Y. Li, F. Xu, M. Zheng, X. Xi, C. Han, A review: the Bioactivities and pharmacological applications of Polygonatum sibiricum polysaccharides, Molecules 23 (5) (2018 May 14) 1170, https://doi.org/10.3390/molecules23051170.
[19] X. Qi, X. Liu, X. Su, C. Xiong, Y. Hao, G. Li, X. Meng, S. Zhang, Effect of Guilu Erxiangao on Alzheimer's disease and its mechanism based on Kidney-brain correlation, Chin. J. Exp. Tradit. Med. Formulae 28 (9) (2022) 158–167.
[20] X. Meng, J. Yan, J. Ma, A.N. Kang, S.Y. Kang, Q. Zhang, C. Lyu, Y.K. Park, H.W. Jung, S. Zhang, Effects of Jowiseungki-tang on high fat diet-induced obesity in mice and functional analysis on network pharmacology and metabolomics analysis, J. Ethnopharmacol. 283 (2022 Jan 30) 114700, https://doi.org/10.1016/j.jep.2021.114700.

[21] X. Meng, X. Zhang, X. Su, X. Liu, K. Ren, C. Ning, Q. Zhang, S. Zhang, Daphnes Cortex and its licorice-processed products suppress inflammation via the TLR4/NF-κB/NLRP3 signaling pathway and regulation of the metabolic profile in the treatment of rheumatoid arthritis, J. Ethnopharmacol. 283 (2022 Jan 30) 114657, https://doi.org/10.1016/j.jep.2021.114657.
[22] Y. Chen, L. Li, C. Hu, X. Zhao, P. Zhang, Y. Chang, Y. Shang, Y. Pang, W. Qian, X. Qiu, H. Zhang, D. Zhang, S. Zhang, Y. Li, Lingguizhugan decoction dynamically regulates MAPKs and AKT signaling pathways to retrogress the pathological progression of cardiac hypertrophy to heart failure, Phytomedicine 98 (2022 Apr) 153951, https://doi.org/10.1016/j.phymed.2022.153951.
[23] M.G. Langille, J. Zaneveld, J.G. Caporaso, D. McDonald, D. Knights, J.A. Reyes, J.C. Clemente, D.E. Burkepile, R.L. Vega Thurber, R. Knight, R.G. Beiko, C. Huttenhower, Predictive functional profiling of microbial communities using 16S rRNA marker gene sequences, Nat. Biotechnol. 31 (9) (2013 Sep) 814–821, https://doi.org/10.1038/nbt.2676.
[24] Y. Hu, M. Yin, Y. Bai, S. Chu, L. Zhang, M. Yang, X. Zheng, Z. Yang, J. Liu, L. Li, L. Huang, H. Peng, An evaluation of Traits, Nutritional, and medicinal component quality of *Polygonatum cyrtonema* Hua and *P. sibiricum* red, Front. Plant Sci. 13 (2022 Apr 18) 891775, https://doi.org/10.3389/fpls.2022.891775.
[25] L.L. Su, X. Li, Z.J. Guo, X.Y. Xiao, P. Chen, J.B. Zhang, C.Q. Mao, D. Ji, J. Mao, B. Gao, T.L. Lu, Effects of different steaming times on the composition, structure and immune activity of Polygonatum Polysaccharide, J. Ethnopharmacol. 310 (2023 Jun 28) 116351, https://doi.org/10.1016/j.jep.2023.116351.
[26] M. Qin, J. Wu, Q. Zhou, Z. Liang, Y. Su, Global cognitive effects of second-generation antidepressants in patients with Alzheimer's disease: a systematic review and meta-analysis of randomized controlled trials, J. Psychiatr. Res. 155 (2022 Nov) 371–379, https://doi.org/10.1016/j.jpsychires.2022.09.039.
[27] H. Niu, I. Álvarez-Álvarez, F. Guillén-Grima, I. Aguinaga-Ontoso, Prevalence and incidence of Alzheimer's disease in Europe: a meta-analysis, Neurologia 32 (8) (2017 Oct) 523–532, https://doi.org/10.1016/j.nrl.2016.02.016. English, Spanish.
[28] P. Scheltens, B. De Strooper, M. Kivipelto, H. Holstege, G. Chételat, C.E. Teunissen, J. Cummings, W.M. van der Flier, Alzheimer's disease, Lancet 397 (10284) (2021 Apr 24) 1577–1590, https://doi.org/10.1016/S0140-6736(20)32205-4.
[29] X. Wang, G. Sun, T. Feng, J. Zhang, X. Huang, T. Wang, Z. Xie, X. Chu, J. Yang, H. Wang, S. Chang, Y. Gong, L. Ruan, G. Zhang, S. Yan, W. Lian, C. Du, D. Yang, Q. Zhang, F. Lin, J. Liu, H. Zhang, C. Ge, S. Xiao, J. Ding, M. Geng, Sodium oligomannate therapeutically remodels gut microbiota and suppresses gut bacterial amino acids-shaped neuroinflammation to inhibit Alzheimer's disease progression, Cell Res. 29 (10) (2019 Oct) 787–803, https://doi.org/10.1038/s41422-019-0216-x.
[30] Z. Breijyeh, R. Karaman, Comprehensive review on Alzheimer's disease: Causes and treatment, Molecules 25 (24) (2020 Dec 8) 5789, https://doi.org/10.3390/molecules25245789.
[31] J. Li, Z. Wang, M. Fan, G. Hu, M. Guo, Potential Antioxidative and anti-Hyperuricemic components targeting superoxide dismutase and Xanthine Oxidase explored from *Polygonatum sibiricum* red, Antioxidants 11 (9) (2022 Aug 25) 1651, https://doi.org/10.3390/antiox11091651.
[32] N. Liu, Z. Dong, X. Zhu, H. Xu, Z. Zhao, Characterization and protective effect of Polygonatum sibiricum polysaccharide against cyclophosphamide-induced immunosuppression in Balb/c mice, Int. J. Biol. Macromol. 107 (Pt A) (2018 Feb) 796–802, https://doi.org/10.1016/j.ijbiomac.2017.09.051.
[33] L. Li, K. Thakur, B.Y. Liao, J.G. Zhang, Z.J. Wei, Antioxidant and antimicrobial potential of polysaccharides sequentially extracted from Polygonatum cyrtonema Hua, Int. J. Biol. Macromol. 114 (2018 Jul 15) 317–323, https://doi.org/10.1016/j.ijbiomac.2018.03.121.
[34] H. Den, X. Dong, M. Chen, Z. Zou, Efficacy of probiotics on cognition, and biomarkers of inflammation and oxidative stress in adults with Alzheimer's disease or mild cognitive impairment - a meta-analysis of randomized controlled trials, Aging (Albany NY) 12 (4) (2020 Feb 15) 4010–4039, https://doi.org/10.18632/aging.102810.
[35] A. Xue, D. Zhao, C. Zhao, X. Li, M. Yang, H. Zhao, C. Zhao, X. Lei, J. Wu, N. Zhang, Study on the neuroprotective effect of Zhimu-Huangbo extract on mitochondrial dysfunction in HT22 cells induced by D-galactose by promoting mitochondrial autophagy, J. Ethnopharmacol. 318 (Pt B) (2024 Jan 10) 117012, https://doi.org/10.1016/j.jep.2023.117012.
[36] W. Wang, S. Li, M. Song, *Polygonatum sibiricum* polysaccharide inhibits high glucose-induced oxidative stress, inflammatory response, and apoptosis in RPE cells, J. Recept. Signal Transduct. Res. 42 (2) (2022 Apr) 189–196, https://doi.org/10.1080/10799893.2021.1883061.